J. Fluid Mech. (1993), *vol.* 247, *pp.* 643–660

Properties of a bidisperse particle–gas suspension Part 2. Viscous relaxation time small compared with collision time

By V. KUMARAN AND DONALD L. KOCH
School of Chemical Engineering, Cornell University, Ithaca, NY 14853, USA

(Received 11 December 1990 and in revised form 24 August 1992)

The properties of a dilute bidisperse particle–gas suspension under low Reynolds number, high Stokes number conditions are studied in the limit $\tau_v \ll \tau_c$, where τ_c is the time between successive collisions of a particle, and τ_v is the viscous relaxation time. In this limit, the particles relax close to their terminal velocity between successive collisions, and we use a perturbation analysis in the small parameter ϵ, which is proportional to τ_v/τ_c, about a base state in which all the particles settle at their terminal velocities. The mean velocities of the two species are $O(\epsilon)$ different from their terminal velocities, and the mean-square velocities are $O(\epsilon)$ smaller than the square of the terminal velocity. The distribution functions for the two species, which incorporate the first effects of collisions between particles settling at their terminal velocities, are derived. The velocity distribution is highly anisotropic in this limit, and the mean-square velocity in the vertical direction is twice that in the horizontal plane. The distribution function for each species is singular at its terminal velocity, and the distributions are non-zero in a finite region in velocity space between the two terminal velocities.

1. Introduction

In this paper, we continue the analysis of a bidisperse suspension of particles settling under gravity in the low Reynolds number, high Stokes number limit, which is applicable to particles of radius 10–100 μm settling in air. In this limit, we can make the following simplifications which permit the analysis of collisions in greater detail: the particle drag is given by Stokes law, the gas inertia is neglected, the interactions between particles are solid-body collisions, and the hydrodynamic interactions between particles are neglected. It is shown in the Appendix that the last approximation is justified in a polydisperse suspension in the high Stokes number limit. The above simplifications make it possible to obtain a detailed understanding of the effect of collisional interactions on the velocity fluctuations in the suspension. It has been postulated that the 'particle pressure' and 'particle diffusion', which are related to the mean-square of the fluctuating velocity, play a crucial role in determining the stability of fluidized beds (Batchelor 1988; Didwania & Homsy 1982). Thus, our analysis will help in understanding the effect of collisions in more complicated systems, such as fluidized beds, where the gas inertia and hydrodynamic interactions may be important.

The distribution of particle velocities is calculated in two asymptotic limits which are defined by the relative magnitudes of two timescales: τ_c, the time between successive collisions of a particle, and τ_v, the viscous relaxation time. In Kumaran &

Koch (1993*a*, which will be referred to as Part 1), the limit $\tau_c \ll \tau_v$, which is equivalent to $St\,V \gg 1$, was analysed. Here, V is the volume fraction of the particles, the Stokes number, St, is $mU/(6\pi\eta a_i^2)$, where m and a_i are the mass and radius of the particle of species i, η is the viscosity of the gas, and U is a characteristic velocity. In this limit, a particle does not experience much deceleration between successive collisions, and the dynamics of the particles resembles that of the molecules of a gas at equilibrium. The leading-order distribution function is an isotropic Gaussian distribution, and is identical to the Maxwell–Boltzmann distribution of molecular velocities.

The limit $\tau_v \ll \tau_c$, which is equivalent to $St\,V \ll 1$, is analysed in this paper. In this limit, we expect the distribution of velocities to be very different from the Maxwell distribution, because the particles relax close to their terminal velocities between successive collisions. We use a perturbation analysis in the small parameter, ϵ, about a base state in which all the particles settle at their terminal velocities. Here, ϵ is the ratio of timescales, τ_v/τ_c, and is proportional to $St\,V$. A distribution function that takes into account the first effect of collisions is calculated, and the mean and mean-square velocities of the particles are evaluated correct to $O(\epsilon^2)$. The analysis in §2 is confined to elastic particles whose drag force is given by Stokes law. Suspensions of inelastic particles are considered in §3, and suspensions in which the drag force is a nonlinear function of the particle velocity are analysed in §4.

2. Suspensions of elastic particles

2.1. *Balance equations*

The system consists of two species, 1 and 2, of spherical elastic particles of radii a_1 and a_2, masses m_1 and m_2 and number densities n_1 and n_2, settling under the influence of gravity in a gas. The terminal velocity of species 1, $v_{1t}^{\dagger}$, is greater than that of species 2, $v_{2t}^{\dagger}$. Here velocity and time variables with superscript $\dagger$ are dimensional, and those without the superscript are scaled variables. In the low Reynolds number limit, the drag force on a particle is given by Stokes law, and is a linear function of the particle velocity. The viscous relaxation time, which is the time constant in Stokes law, is given by

$$\tau_{vi} = m_i/\mu_i, \tag{2.1}$$

where μ_i is $6\pi\eta a_i$. The velocities are scaled by the difference in the terminal velocities, $v_{1t}^{\dagger}-v_{2t}^{\dagger}$, and the time variable is scaled by the viscous relaxation time, τ_{v1}. To simplify the algebra, we define a new velocity variable, $\boldsymbol{u}_i$, as $(\boldsymbol{v}_i - v_{it}\boldsymbol{e}_z)$, the difference between the particle velocity and its terminal velocity. The acceleration of a particle can be expressed in terms of $\boldsymbol{u}_i$ as

$$\frac{\mathrm{d}\boldsymbol{u}_i}{\mathrm{d}t} = -\boldsymbol{u}_i(\tau_{v1}/\tau_{vi}). \tag{2.2}$$

The two timescales that govern the suspension dynamics are the viscous relaxation time τ_{vi}, defined in (2.1), and the collision time τ_{cij}, which is the time between successive collisions of a particle of species i with particles of species j. The expression for the collision time was given in (2.2) in Part 1. In this paper, the fluctuating velocity of the particles is of the same order of magnitude as the difference in their terminal velocities, and the collision time is

$$\tau_{cij} = 1/[n_j \pi d_{ij}^2 (v_{1t}^{\dagger} - v_{2t}^{\dagger})]. \tag{2.3}$$

Here d_{ij} is the sum of the radii of species i and j. The parameter ϵ used in the perturbation analysis is defined as the ratio of the timescales:

$$\epsilon = \tau_{v1}/\tau_{c12}. \tag{2.4}$$

The conservation equation for the distribution function is

$$\frac{\partial f_i}{\partial t} = -\nabla_{\boldsymbol{u}_i}\cdot\left(\frac{\mathrm{d}\boldsymbol{u}_i}{\mathrm{d}t} f_i\right) + \frac{\partial_c f_i}{\partial t}. \tag{2.5}$$

The first and second terms on the right-hand side represent the change in the distribution function due to viscous forces, and the change in the distribution function due to collisional interactions, respectively. The latter term is identical to the Boltzmann collision integral in the case of elastic particles. For convenience, the collision integral is divided into two parts:

$$\frac{\partial_c f_i}{\partial t} = N_i^{\mathrm{in}}(\boldsymbol{u}_i) - N_i^{\mathrm{out}}(\boldsymbol{u}_i). \tag{2.6}$$

Here, the collisional accumulation, $N_i^{\mathrm{in}}(\boldsymbol{u}_i)$, is the number of particles scattered into the differential volume $\mathrm{d}\boldsymbol{u}_i$ per unit time due to collisions between particles outside this volume, and the collisional depletion, $N_i^{\mathrm{out}}(\boldsymbol{u}_i)$, is the number of particles scattered out of $\mathrm{d}\boldsymbol{u}_i$ per unit time due to collisions involving a particle in this volume. The conservation equation is the same as the Boltzmann equation used in kinetic theory of gases, except for the important difference that the particle's acceleration is dependent on its velocity. This analysis is in the limit where the particles relax to their terminal velocity between collisions, so the distribution function can be significantly different from the Maxwell–Boltzmann distribution.

The balance equations for the moments of $\boldsymbol{u}_i$ are obtained by multiplying (2.5) by the velocity and the square of the velocity and integrating over the domain of $\boldsymbol{u}_i$. The steady-state balance equations for the moments of u_{iz}, the velocity in the vertical direction, and u_{ir}, the magnitude of the velocity in the horizontal plane, analogous to (2.21) in Part 1, are

$$-(\tau_{v1}/\tau_{vi})\langle u_{iz}\rangle + \partial_c\langle u_{iz}\rangle/\partial t = 0, \tag{2.7a}$$

$$-2(\tau_{v1}/\tau_{vi})\langle u_i^2\rangle + \partial_c\langle u_i^2\rangle/\partial t = 0, \tag{2.7b}$$

$$-2(\tau_{v1}/\tau_{vi})\langle u_{ir}^2\rangle + \partial_c\langle u_{ir}^2\rangle/\partial t = 0. \tag{2.7c}$$

Here, $\partial_c\langle\beta_i\rangle/\partial t$ is the change in the moment $\langle\beta_i\rangle$ due to collisions, and the factor τ_{v1}/τ_{vi} appears because the time variable is scaled by τ_{v1}. The momentum and energy balance equations at steady state for the suspension are

$$n_1 m_1\langle u_{1z}\rangle/\tau_{v1} + n_2 m_2\langle u_{2z}\rangle/\tau_{v2} = 0, \tag{2.8a}$$

$$n_1 m_1(\langle u_{1z}\rangle v_{1t} + \langle u_1^2\rangle)/\tau_{v1} + n_2 m_2(v_{2t}\langle u_{2z}\rangle + \langle u_2^2\rangle)/\tau_{v2} = 0. \tag{2.8b}$$

From the above relations, it can be shown that the mean velocities of the two species are between the two terminal velocities:

$$v_{1t} > (v_{1t} + \langle u_{1z}\rangle) > (v_{2t} + \langle u_{2z}\rangle) > v_{2t}. \tag{2.9}$$

2.2 *Leading-order velocity moments*

In the limit $\tau_{vi} \ll \tau_{cij}$, the particles relax close to their terminal velocities between successive collisions, and the fraction of particles that have velocities significantly different from the terminal velocities is small at any point in time. To obtain the leading-order collisional change in the mean and mean-square velocities, we assume

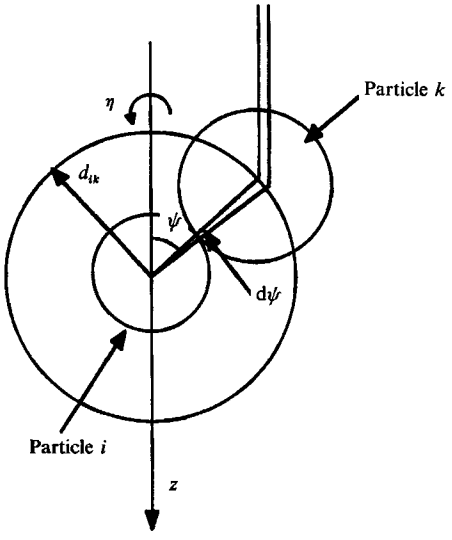

FIGURE 1. Coordinate system for analysing a collision between particles moving at their terminal velocities.

that the velocities of colliding particles are equal to their terminal velocities. The collisional configuration is shown in figure 1. Here, ψ and η are the azimuthal and meridional angles made by the impact vector, which is the vector joining the centres of the particles at the point of collision. The frequency of collisions of a particle of species i with particles of the other species $k = 3-i$, such that the impact vector is in the differential solid angle $\sin\psi\,\mathrm{d}\psi\,\mathrm{d}\eta$ about (ψ, η), is given by

$$\text{frequency of collisions} = \epsilon(\tau_{c12}/\pi\tau_{cik})\cos\psi\sin\psi\,\mathrm{d}\psi\,\mathrm{d}\eta. \tag{2.10}$$

The factor ϵ appears in (2.10) because the collision frequency is scaled by the viscous relaxation time τ_{v1}. The velocities of the particles are expressed in terms of the velocity of the centre of mass, $\boldsymbol{q}$, and the velocity difference, $\boldsymbol{w}$. The horizontal components of $\boldsymbol{q}$ and $\boldsymbol{w}$ are zero because we assume the particles are settling at their terminal velocities, and their vertical components are given by

$$q_z = \frac{m_1 v_{1t} + m_2 v_{2t}}{m_1 + m_2}, \quad w_z = (-1)^{i-1}. \tag{2.11a, b}$$

Note that all velocities are scaled by the difference in terminal velocities and i is 1 for the heavier species. The velocity of the centre of mass, $\boldsymbol{q}$, remains unchanged in a collision owing to the momentum conservation condition. The components of the velocity difference between the particles after the collision are

$$w_z^* = (-1)^{i-1}(\sin^2\psi - e\cos^2\psi), \quad w_r^* = \tfrac{1}{2}(e+1)\sin(2\psi), \tag{2.12a, b}$$

where e is the coefficient of restitution. In this section we consider elastic particles, for which the coefficient of restitution is 1. The change in the mean and mean-square velocities of the particles for an elastic collision are

$$\Delta u_{iz} = (-1)^i \frac{m_k}{m_i + m_k}(2\cos^2\psi), \quad \Delta(u_i^2) = (-1)^i \left(\frac{m_k}{m_i + m_k}\right)^2 (4\cos^2\psi), \tag{2.13a, b}$$

$$\Delta(u_{ir}^2) = \left(\frac{m_k}{m_i + m_k}\right)^2 \sin^2(2\psi). \tag{2.13c}$$

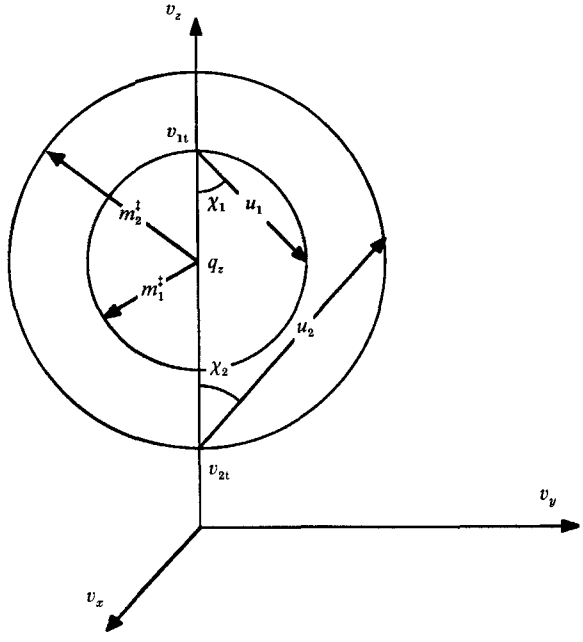

FIGURE 2. Spherical coordinate systems in velocity space used for solving the conservation equation for the distribution function.

The rate of change of a function of the velocity, $\beta_i(\boldsymbol{u}_i)$, is calculated by integrating the product of the collision frequency, (2.10), and the change in the property during a collision, $\Delta\beta_i$, (2.13), in the ψ-coordinate from 0 to $\frac{1}{2}\pi$ and in η from 0 to 2π:

$$\frac{\partial_c\langle\beta_i\rangle}{\partial t} = \epsilon\left(\frac{\tau_{c12}}{\pi\tau_{cik}}\right)\int_{\eta=0}^{2\pi}\int_{\psi=0}^{\frac{1}{2}\pi}\Delta\beta_i\cos\psi\sin\psi\,\mathrm{d}\psi\,\mathrm{d}\eta. \tag{2.14}$$

The mean and mean-square velocities are calculated by substituting the collisional changes into the balance equations (2.7):

$$\langle u_{iz}\rangle = (-1)^i\epsilon\gamma_{ik}\left(\frac{m_k}{m_i+m_k}\right), \quad \langle u_i^2\rangle = \epsilon\gamma_{ik}\left(\frac{m_k}{m_i+m_k}\right)^2, \tag{2.15a, b}$$

$$\langle u_{ir}^2\rangle = \tfrac{1}{3}\epsilon\gamma_{ik}\left(\frac{m_k}{m_i+m_k}\right)^2, \tag{2.15c}$$

where γ_{ik} is an $O(1)$ factor, and is given by

$$\gamma_{ik} = (\tau_{vi}/\tau_{v1})\,(\tau_{c12}/\tau_{cik}). \tag{2.15d}$$

From (2.15*b*, *c*) it can be seen that the velocity distribution is highly anisotropic, since the mean-square of the vertical fluctuating velocity is twice the fluctuating velocity in the horizontal plane. Note that in an isotropic distribution, the mean-square of the vertical fluctuating velocity is half that of the fluctuating velocity in the horizontal plane.

2.3. *Velocity distribution function*

In this section, a perturbation analysis is used to calculate the velocity distribution functions that take into account the first effect of particle collisions. First, the accumulation and depletion in velocity space, $N_i^{\mathrm{in}}(\boldsymbol{u}_i)$ and $N_i^{\mathrm{out}}(\boldsymbol{u}_i)$ in (2.6), due to

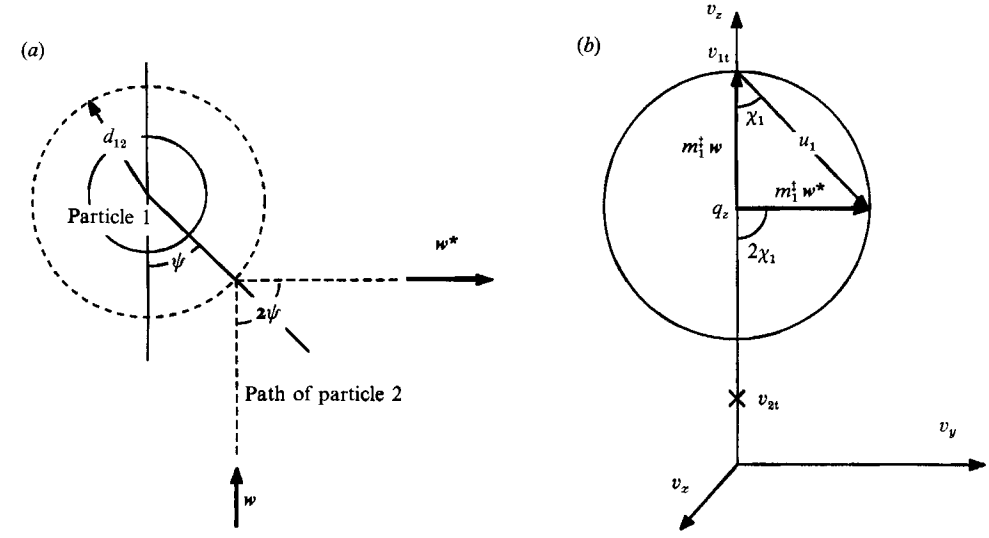

FIGURE 3. Relation between the angular coordinates of the impact vector and the angular displacement of the relative velocity vector during the collision. (*a*) Real space, (*b*) velocity space.

collisions between particles settling at their terminal velocities, are calculated. These are substituted into the conservation equation (2.5), which is solved for the distribution functions.

The gravitational and viscous forces transport a particle towards its terminal velocity (see (2.2)). This symmetry in the particle trajectories can be exploited by using two spherical coordinate systems centred at the terminal velocities of the two species, as shown in figure 2. The radial, azimuthal and meridional coordinates in these systems are u_i, χ_i and ι_i, respectively. Since the motion of the particles is along the radial coordinate, the conservation equation, at steady state, reduces to the form:

$$-\left(\frac{\tau_{v1}}{\tau_{vi}}\right)\left(\frac{1}{u_i^2}\right)\left[\frac{\partial}{\partial u_i}[u_i^3 f_i(u_i, \chi_i, \iota_i)]\right] = N_i^{in}(u_i, \chi_i, \iota_i) - N_i^{out}(u_i, \chi_i, \iota_i). \tag{2.16}$$

The collisional terms are calculated by relating the angles χ_i and ι_i in velocity space to the angular coordinates of the impact vector (ψ and η in figure 1). As shown in figure 3, the angle between the relative velocity vectors before and after collision is 2ψ. In velocity space, the same angle is $2\chi_i$. Therefore, the angles ψ and χ_i are equal. It is easy to see that the meridional angle in velocity space, ι_i, is the same as the meridional angle of the impact vector, η. Thus, the relationships between the angles in real and velocity space are

$$\psi = \chi_i, \quad \eta = \iota_i. \tag{2.17a, b}$$

From (2.12) and (2.17), the velocities of the particles after a collision are

$$u_{ix}^* = 2m_i^\dagger \cos\chi_i \sin\chi_i \cos\iota_i, \quad u_{iy}^* = 2m_i^\dagger \cos\chi_i \sin\chi_i \sin\iota_i, \tag{2.18a, b}$$

$$u_{iz}^* = (-1)^i 2m_i^\dagger \cos^2\chi_i, \tag{2.18c}$$

where $m_i^\dagger = m_k/(m_i+m_k)$. The velocities after collision, (2.18), lie on a sphere, S_i, of radius $m_i^\dagger$, centred at the common velocity $\mathbf{q}$, which is given by (2.12*a*). The equation of the sphere is

$$u_i = 2m_i^\dagger \cos\chi_i. \tag{2.19}$$

Note that the origin of the coordinate system is at v_{it} (see figure 3*b*). Particles are transported onto the surface S_i by collisions, and they move back towards the terminal velocity owing to viscous and gravitational forces. The collisional accumulation on S_i, calculated from the frequency of collisions, (2.10), and the relation between the angles in real and velocity space, (2.17), is

$$N_i^{\text{in}}(u_i, \chi_i, \iota_i) = \epsilon\left(\frac{\tau_{c12}}{\tau_{cik}}\right)\frac{1}{4\pi m_i^{\dagger 2}\cos\chi_i}\delta(u_i - 2m_i^{\dagger}\cos\chi_i). \tag{2.20}$$

The collisional accumulation is a delta function on the surface of the sphere S_i, and, therefore, there is a step change in the distribution function at this surface.

There is collisional depletion, $N_i^{\text{out}}(\boldsymbol{u}_i)$, due to collisions involving a particle in the volume $\mathrm{d}\boldsymbol{u}_i$ with a particle of the other species $k = 3-i$. It can be shown that an expression for $N_i^{\text{out}}(\boldsymbol{u}_i)$, which is correct to leading order in small ϵ, is obtained by setting the relative velocity equal to the difference in the terminal velocities. The distribution function, which is calculated later in this section, consists of an 'inner region', where u_k is $O(\exp(-1/\epsilon))$ and the fraction of the particles is $(1-O(\epsilon))$; and an 'outer region', where u_k is $O(1)$ and the fraction of particles is $O(\epsilon)$. Thus, we make an $O(\epsilon)$ error by approximating the relative velocity when particle i is in the inner region and, using this approximation, the collisional depletion for species i in the inner region is

$$N_i^{\text{out}}(\boldsymbol{u}_i) = \epsilon(\tau_{c12}/\tau_{cik})f_i(\boldsymbol{u}_i). \tag{2.21}$$

When particle i is in the outer region, there is a large relative error in the collisional depletion if we replace the particle velocities by their terminal velocities. However, the net depletion due to collisions is $O(\epsilon)$ smaller than that due to drag forces in this region. Thus, the error made by using (2.21) in the conservation equation (2.16) is small throughout the velocity domain.

Substituting the equation for the collisional depletion, (2.21), into the conservation equation in velocity space, (2.16), we get

$$\left(\frac{\tau_{v1}}{\tau_{vi}}\right)u_i\frac{\partial}{\partial u_i}[f_i(u_i, \chi_i, \iota_i)] + \left[3\left(\frac{\tau_{v1}}{\tau_{vi}}\right) - \epsilon\left(\frac{\tau_{c12}}{\tau_{cik}}\right)\right]f_i(u_i, \chi_i, \iota_i) = -N_i^{\text{in}}(u_i, \chi_i, \iota_i). \tag{2.22}$$

Since the collisional accumulation is a delta function on the surface S_i bounding the velocity domain, we can solve the differential equation by setting the right-hand side of (2.22) equal to zero within the domain bounded by S_i to obtain

$$f_i = c(\chi_i)\, u_i^{\epsilon\gamma_{ik}-3}. \tag{2.23}$$

The function $c(\chi_i)$ is determined from the condition that the distribution function undergoes the following step change on the surface S_i due to the collisional accumulation:

$$f_i|_{u_i=2m_i^{\dagger}\cos\chi_i^{+}} - f_i|_{u_i=2m_i^{\dagger}\cos\chi_i^{-}} = \frac{-\epsilon\gamma_{ik}}{8\pi m_i^{\dagger 3}\cos^2\chi_i}. \tag{2.24}$$

Using this boundary condition and the fact that f_i is zero outside S_i, the constant $c(\chi_i)$ in (2.23) is

$$c(\chi_i) = (\epsilon\gamma_{ik}/\pi)\,(\cos\chi_i)^{1-\epsilon\gamma_{ik}}\,(2m_i^{\dagger})^{-\epsilon\gamma_{ik}}. \tag{2.25}$$

This completes the calculation of the velocity distribution functions that take into account the first effect of particle collisions. The distribution function for species i is singular at its terminal velocity, but it is integrable over the velocity domain and

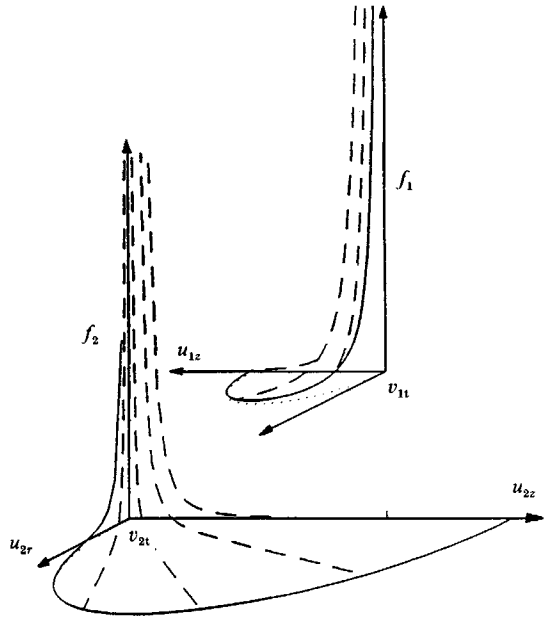

FIGURE 4. Schematic of the shape of the distribution function in a bidisperse suspension. The zero levels of the distribution functions of the two species have been separated for clarity. The dotted line represents the projection of the surface S_i onto the (u_r, u_z)-plane, and the solid line shows the distribution function on this surface.

is normalized. Figure 4 is a schematic of the shape of the distribution function. The zero reference levels of the distribution functions of the two species have been separated for clarity. Figure 5 is a contour plot of the distribution functions for a suspension in which the ratio of particle radii, a_2/a_1, is 0.7, and the ratio of timescales, ϵ, is 0.1. The form of the distribution function confirms the existence of the inner and outer regions discussed above. In the 'inner region', u_i is $O(\exp(-1/\epsilon))$ and the fraction of the particles is $1-O(\epsilon)$. In the 'outer region', u_i is $O(1)$ and the distribution function is $O(\epsilon)$. There is a collisional depletion of particles in the inner region due to collisions between particles travelling close to their terminal velocities, which is balanced by an accrual due to drag forces. There is no leading-order collisional accumulation in this region. The particles are displaced onto the surface S_i owing to collisions, and are transported through the outer region owing to viscous drag forces. The collisional accumulation and depletion are $O(\epsilon)$ smaller than the viscous accumulation in the outer region.

2.4 *First correction to the velocity moments*

The first correction to the velocity moments is calculated using the distribution function derived in §2.3. We distinguish between three types of collisions depending on the velocities of colliding particles:

(i) Collisions between two particles that are in the inner region. The frequency of these collisions is $O(n_i n_k/\tau_{cik})$.

(ii) Collisions in which one of the particles is in the inner region and the other is in the outer region, which occur with a frequency of $O(\epsilon n_i n_k/\tau_{cik})$.

(iii) Collisions in which both the particles are in the outer region. The frequency of these collisions is $O(\epsilon^2 n_i n_k/\tau_{cik})$.

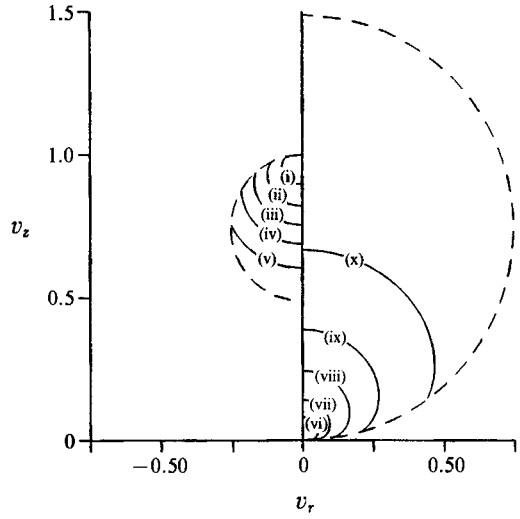

FIGURE 5. Contour plots of distribution functions of species 1 and 2 in a suspension. The size ratio, a_2/a_1, is 0.7, the ratio of the number densities, n_2/n_1, is 1.0, and the ratio of time scales, ϵ, is 0.1. The solid lines are contours of equal distribution function f_i, and the broken line is the boundary of the domain of the distribution function. The velocities are non-dimensionalized by the difference between the terminal velocities of the two species, and the origin of the velocity coordinate in the vertical direction is at the terminal velocity of species 2. The values of the distribution function on the different contours are: Species 1: (i) 25.0, (ii) 5.0, (iii) 2.0, (iv) 1.0, (v) 0.25. Species 2: (vi) 25.0, (vii) 5.0, (viii) 1.0, (ix) 0.25, (x) 0.05.

Collisions of the first kind cause the leading-order collisional change in the velocity moments, which was calculated in §2.2. Those of the second kind contribute to the first correction to the collisional terms, which is calculated in the following manner. First, assume the particles of species 1 are at their terminal velocity, and calculate the momentum and energy transferred due to collisions with particles of species 2 that have a distribution of velocities given by (2.23) and (2.25). To this add the transfers due to collisions between particles of species 2 settling at their terminal velocities and particles of species 1 having a velocity distribution given by (2.23) and (2.25). It can be easily seen that this average is equal to the sum of the first correction and twice the leading-order transfers. Therefore, the collisional terms correct to $O(\epsilon^2)$ are calculated by subtracting the leading-order terms from the average described above. The collisional change in the moment $\langle\beta_i\rangle$ due to collisions between particles of species i and k, correct to $O(\epsilon^2)$, is

$$\left(\frac{\partial_c\langle\beta_i\rangle}{\partial t}\right)_{ik} = \frac{\epsilon}{\pi}\left(\frac{\tau_{c12}}{\tau_{cik}}\right)\left[\int_{\eta=0}^{2\pi}\int_{\psi=0}^{\frac{1}{2}\pi}\int_{u_i}\Delta_{ik}(\beta_i)f_i(\boldsymbol{u}_i)\,w\cos\psi\sin\psi\,\mathrm{d}\mathbf{u}_i\,\mathrm{d}\psi\,\mathrm{d}\eta\right.$$
$$+\int_{\eta=0}^{2\pi}\int_{\psi=0}^{\frac{1}{2}\pi}\int_{u_k}\Delta_{ki}(\beta_i)f_k(\boldsymbol{u}_k)\,w\cos\psi\sin\psi\,\mathrm{d}\boldsymbol{u}_k\,\mathrm{d}\psi\,\mathrm{d}\eta$$
$$\left.-\int_{\eta=0}^{2\pi}\int_{\psi=0}^{\frac{1}{2}\pi}\Delta\beta_i(\boldsymbol{u}_i)\cos\psi\sin\psi\,\mathrm{d}\psi\,\mathrm{d}\eta\right]. \tag{2.26}$$

Here k is $3-i$, $\Delta_{ik}(\beta_j)$ is the change in the property β_j of particle j due to a collision between a particle moving at the velocity $\boldsymbol{u}_i$ and a particle of species k moving at its terminal velocity, where j can be either i or k. $\Delta\beta_i$ is the leading order change in the

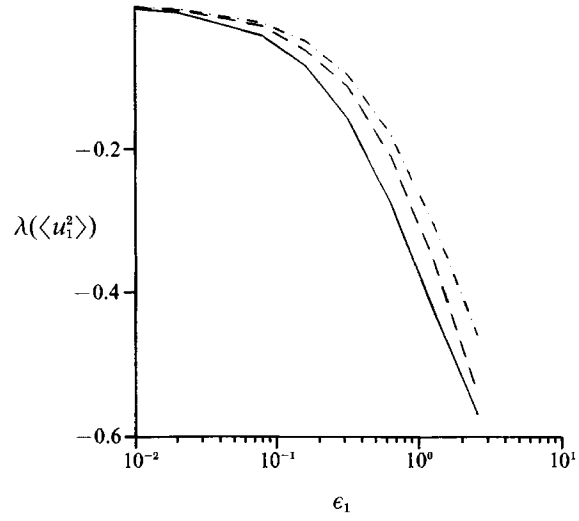

FIGURE 6. $\lambda(\langle u_1^2 \rangle)$, which is the ratio of the $O(\epsilon^2)$ correction to the mean-square velocity to the leading-order term given in (2.15*b*), as a function of ϵ_1. The ratio of number densities is 1, and the densities of the particles of the two species are equal. The ratio of particle sizes $a_c = a_2/a_1$ is −·−·−·−·, $a_c = 0.5$; ——, $a_c = 0.7$; − − − − − − −, $a_c = 0.9$.

velocity moments given in (2.13). The collisional change in the mean vertical velocity, u_{iz}, and the mean-square velocity, u_i^2, are proportional to the rate of momentum and energy transfer in collisions. Since elastic collisions conserve momentum and total energy, there is no change in these velocity moments due to collisions between particles of the same species, and the collisional rate of change of these moments can be calculated using (2.26). However, there is a redistribution of energy between the horizontal and vertical direction due to collisions between particles of the same species, and this causes a change in the mean-square horizontal velocity, u_{ir}^2, due to collisions of this type. This contribution is given by

$$\left(\frac{\partial_c \langle u_{ir}^2 \rangle}{\partial t}\right)_{ii} = \frac{\epsilon}{\pi}\left(\frac{\tau_{c12}}{\tau_{cii}}\right)\int_{\eta=0}^{2\pi}\int_{\psi=0}^{\frac{1}{2}\pi}\int_{\boldsymbol{u}_i}\Delta_{ii}(u_{ir}^2) f_i(\boldsymbol{u}_i)\, w \cos\psi \sin\psi \, \mathrm{d}\boldsymbol{u}_i \, \mathrm{d}\psi \, \mathrm{d}\eta. \quad (2.27)$$

Here $\Delta_{ii}(u_{ir}^2)$ is the change in u_{ir}^2 in a collision between one particle travelling at $\boldsymbol{u}_i$ and another travelling at its terminal velocity. The $O(\epsilon^2)$-correct mean and mean-square velocities are calculated by substituting the collisional transfer rates, (2.26) and (2.27), into the balance equations, (2.7).

Some of the effects of variations in ϵ and the ratio of particle radii on the velocity moments of particles of species 1 are shown in figures 6 and 7. In these figures, the number densities of the particles of the two species are equal, and the densities of the solid in the particles are also equal. The dimensionless parameter ϵ_1 is given by $[n_1(4\pi a_1^2) v_{1t}^{\dagger}/\tau_{v1}]$. The parameter ϵ_1 has the same form as ϵ, but depends only on the terminal velocity of species 1, and not on the difference in the terminal velocities. This helps illustrate the effect of changing the radius and number density of species 2. Note that ϵ_1 is equal to $3St_1 V_1$, where St_1 and V_1 are the Stokes number and volume fraction of particles of species 1.

Figure 6 shows $\lambda(\langle u_1^2 \rangle)$, which is the ratio of the $O(\epsilon^2)$ correction and the leading-order mean-square velocity, as a function of ϵ_1. The leading-order term is given by (2.15*b*), and the $O(\epsilon^2)$ correction is calculated using (2.26). The corresponding ratios

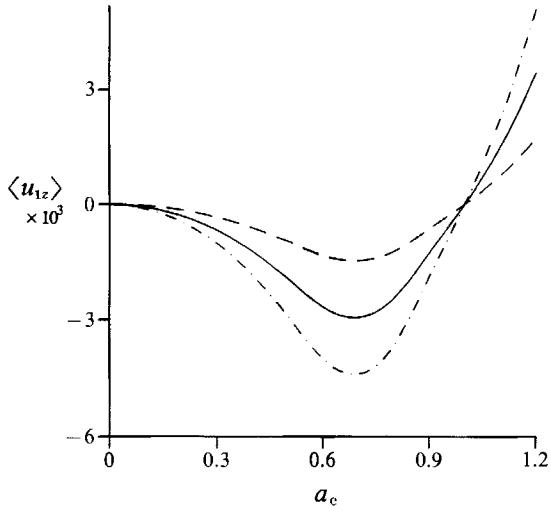

FIGURE 7. Difference between the mean velocity and the terminal velocity of particles of species 1, non-dimensionalized by $v_{1t}^{\dagger}$, as a function of the size ratio $a_c = a_2/a_1$ for various values of number density ratios $n_c = n_2/n_1$. The densities of the particles of the two species are equal, and ϵ_1 is 0.05. ————, $n_c = 0.5$; ——, $n_c = 1.0$; –·–·–·–·–, $n_c = 1.5$.

for the other moments show similar trends. The $O(\epsilon^2)$ correction is less than 0.1 times the leading-order term for $\epsilon_1 \leqslant 0.3$, and it is half the leading-order term at $\epsilon_1 = 2.5$. This indicates that the asymptotic analysis is quite robust in this limit, and it can be used to calculate the velocity moments at moderately small values of ϵ_1. Another salient feature is that the $O(\epsilon^2)$ corrections to the velocity moments tend to reduce their magnitude. These corrections are due to the collisional dispersion of particle velocities between their terminal velocities, which has a two-fold effect on the collisional transfer of momentum and energy. First, it decreases the difference in the momentum and energy of colliding particles, reducing the transfer of momentum and energy in each collision. Second, it decreases the relative velocity between the particles at the point of collision, thereby decreasing the frequency of collisions.

Figure 7 shows the variation of $\langle u_{1z} \rangle$ as a function of the ratio of particle radii, a_2/a_1. The number densities of the two species are equal, and the parameter ϵ_1 is 0.05. As the radius of species 2 is increased, the magnitudes of the mean and mean-square velocities of species 1 first increase and then decrease. These trends can be explained as follows. The initial increase in the radius of species 2 from zero results in an increase in its momentum and energy at the point of collision, and the collisional transfer rates of momentum and energy increase. As the radius of species 2 is further increased, however, the difference between the terminal velocities of the two species decreases, and the frequency of collisions decreases, causing a decrease in the collisional transfer rates. As the size ratio is increased above one, both the momentum of particles of species 2 and the difference in terminal velocities increase, and there is a marked increase in the velocity moments.

3. Suspensions of inelastic particles

Inelastic collisions between particles provide an additional mechanism for the dissipation of energy. In the limit $\tau_c \ll \tau_v$ ($St\,V \gg 1$), analysed in Part 1, the energy dissipation due to inelastic collisions is large compared to that due to drag forces as

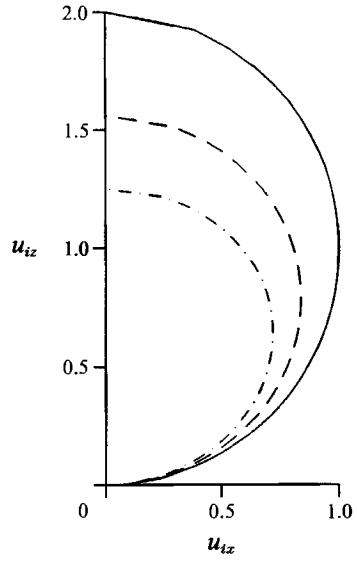

FIGURE 8. Domain of the velocity distribution function for different values of the coefficient of restitution, e. The velocity coordinates are scaled by the maximum particle velocity in the horizontal direction in an elastic suspension. -·-·-·-·-, $e = 0.5$; ————, $e = 0.75$; ——, $e = 1.0$.

long as $(St\,V)^{-\frac{2}{3}} \ll \delta$, where $\delta = 1-e^2$. Thus, inelastic collisions can significantly decrease the magnitude of the velocity fluctuations even when the coefficient of restitution, e, is close to 1.

In the limit $\tau_v \ll \tau_c$, the dissipation of energy due to inelastic collisions is $O(\delta m_i(v_{1t}^{\dagger}-v_{2t}^{\dagger})^2/\tau_c)$, which is $O(\delta)$ smaller than the dissipation due to drag forces. Thus, inelastic collisions cause an $O(\delta)$ change in the magnitude of the fluctuating velocities, which is small for $\delta \ll 1$. However, unlike the analysis in Part 1, the present analysis for $\tau_v \ll \tau_c$ is not limited to small δ. The magnitude of the velocity difference between the particles after a collision is given by (2.12), and the mean and mean-square velocities are

$$\langle u_{iz}\rangle = (-1)^i \epsilon\gamma_{ik}\left(\frac{m_k}{m_i+m_k}\right)\left(\frac{e+1}{2}\right), \quad \langle u_i^2\rangle = \epsilon\gamma_{ik}\left(\frac{m_k}{m_i+m_k}\right)^2\left(\frac{e(e+1)}{2}\right), \tag{3.1a, b}$$

$$\langle u_{ir}^2\rangle = \epsilon\gamma_{ik}\left(\frac{m_k}{m_i+m_k}\right)^2\frac{(e+1)^2}{12}. \tag{3.1c}$$

The distribution function for an inelastic suspension is calculated by a procedure similar to that used for an elastic suspension in §2.3. The relations between the angular coordinates of the impact vector, (ψ,η), and the velocity vector after collision, (χ_i,ι_i), are given by (2.17). The velocity of a particle after collision is, instead of (2.18):

$$u_{ix}^* = (e+1)\,m_i^{\dagger}\cos\chi_i\sin\chi_i\cos\iota_i, \tag{3.2a}$$

$$u_{iy}^* = (e+1)\,m_i^{\dagger}\cos\chi_i\sin\chi_i\sin\iota_i, \tag{3.2b}$$

$$u_{iz}^* = (-1)^i\,m_i^{\dagger}(-1+\sin^2\chi_i-e\cos^2\chi_i). \tag{3.2c}$$

The surface, S_i, onto which the particles are displaced after collision, is given by

$$u_i = m_i^{\dagger}[\tfrac{1}{2}(e+1)\sin^2(2\chi_i)+(\sin^2\chi_i-e\cos^2\chi_i-1)^2]^{\frac{1}{2}} = u_{is}(\chi_i) \tag{3.3}$$

and the collisional accumulation is given by

$$N_i^{\text{in}}(u_i, \chi_i, \iota_i) = \epsilon\left(\frac{\tau_{c12}}{\tau_{cik}}\right)\frac{\cos\chi_i}{\pi(u_{is})^2}\delta(u_i - u_{is}). \tag{3.4}$$

The distribution function in the region bounded by S_i is given by (2.23). However, the constant $c(\chi_i)$ in this expression is, instead of (2.25),

$$c(\chi_i) = \frac{\epsilon\gamma_{ik}}{\pi}(\cos\chi_i)(u_{is})^{-\epsilon\gamma_{ik}}. \tag{3.5}$$

The qualitative form of the distribution function is the same as that for a suspension of elastic particles. However, its domain is smaller, since the velocity of the particle after an inelastic collision is smaller than that after an elastic collision. The shape of the surface, S_i, which bounds the domain of the distribution function, is shown in figure 8 for different values of the coefficient of restitution, e.

4. Suspensions of particles with nonlinear drag

In this section, we examine the effect of a nonlinear pseudo-steady drag force on the velocity distribution. In general, at non-zero Reynolds number, the particle drag is nonlinear in its velocity, and depends on the time history of the particle velocity as well. However, for Reynolds number less than about 10 (particles of diameter less than about 400 μm settling in air), the dependence of the drag force on the time history of the particle velocity can be neglected (see Lumley 1978). We assume that the acceleration of the particles due to gravitational and viscous forces is of the form

$$\frac{\mathrm{d}\boldsymbol{u}_i}{\mathrm{d}t} = -\left(\frac{\tau_{v1}}{\tau_{vi}}\right)\frac{\boldsymbol{u}_i}{u_i}h_i(u_i), \tag{4.1}$$

where $h_i(u_i)$ is a dimensionless function of the difference between the particle velocity and its terminal velocity. The non-dimensional conservation equation in velocity space is

$$-\left(\frac{\tau_{v1}}{\tau_{vi}}\right)\nabla_{u_i}\cdot\left(\frac{\boldsymbol{u}_i}{u_i}h(u_i)f_i\right) = N_i^{\text{in}}(\boldsymbol{u}_i) - N_i^{\text{out}}(\boldsymbol{u}_i). \tag{4.2}$$

We cannot obtain a closed set of balance equations for the velocity moments by averaging the product of (4.2) with the velocity and square of the velocity. However, these moments can be calculated by first deriving the velocity distribution function and then taking its moments. The method for calculating the velocity distribution function is outlined below.

The collisional accumulation and depletion are given by (2.20) and (2.21), respectively. We solve the equations in the spherical coordinate systems shown in figure 2. There is an accumulation of particles on the sphere, S_i, described by (2.19). Within this sphere, the conservation equation, analogous to (2.16), is

$$\frac{\partial f_i}{\partial u_i} = -\frac{f_i}{h(u_i)}\left[\frac{\partial[h(u_i)]}{\partial u_i} + \frac{2h(u_i)}{u_i} + N_i^{\text{in}}(\boldsymbol{u}_i) - \epsilon\gamma_{ik}\right]. \tag{4.3}$$

This is solved using the boundary condition (2.24) at the surface S_i.

For example, if the drag on a particle is proportional to the mth power of the velocity, where m is any real number

$$h(u_i) = u_i^m, \tag{4.4}$$

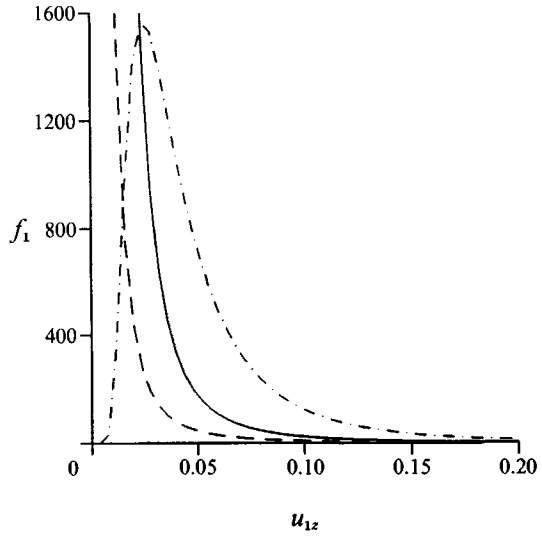

FIGURE 9. Velocity distribution function f_1, as a function of u_1 at $\chi_1 = 0$, for suspensions with nonlinear drag for various values of m. The size ratio, a_2/a_1, is 0.8, and ϵ is 0.1. The dependence of the drag force on the index m is given by (4.1) and (4.4). ————, $m = 0.5$; ——, $m = 1.0$; –·–·–·–, $m = 2.0$.

the solution for the distribution function is given by

$$f_i = u_i^{-(m+2)} \exp\left(-\frac{\epsilon\gamma_{ik}}{(m-1)\,u_i^{(m-1)}}\right) c(\chi_i). \tag{4.5}$$

The constant $c(\chi_i)$, calculated using (2.24), is

$$c(\chi_i) = \frac{\epsilon\gamma_{ik}}{\pi} \cos\chi_i \exp\left[\frac{\epsilon\gamma_{ik}}{(m-1)\,(2m_i^{\ddagger}\cos\chi_i)^{(m-1)}}\right]. \tag{4.6}$$

Note that this distribution function is normalized.

The structure of the distribution function (4.6) differs from that for a suspension which obeys the linear drag law. For $m > 1$, the distribution function is zero at the origin, but increases steeply and reaches a maximum of $O[(\epsilon\gamma_{ik})^{-3/(m-1)}]$ at $u_i = [(\epsilon\gamma_{ik}/(m+2))^{(1/(m-1))}]$. For $m < 1$, the distribution function is singular at the origin, and decreases as u_i increases. In the outer region, where u_i is $O(1)$, the distribution function is $O(\epsilon)$. The distribution function f_1 as a function u_1 at $\chi_1 = 0$, which corresponds to the velocity in the vertical direction, is shown in figure 9 for $m = 0.5$, 1.0 and 2.0.

5. Conclusions

In this paper, we have presented an analysis of a bidisperse suspension of particles settling in a gas in the limit where the viscous relaxation time, τ_v, is small compared to the time between collisions, τ_c. In this limit, a particle relaxes to its terminal velocity between collisions, and we use a perturbation analysis in the small parameter ϵ about a base state in which all the particles settle at their terminal velocities. Here, ϵ is the ratio of timescales τ_v/τ_c, and is proportional to $St\,V$, so this analysis is valid in the limit $St\,V \ll 1$. The first corrections to the velocity moments

are $O(\epsilon)$ when scaled by the difference in terminal velocities, and these are calculated by averaging over the orientations of the impact vector. The distribution of velocities is highly anisotropic, and the mean-square of the fluctuating velocity in the vertical direction is twice that in the horizontal plane. This is very different from the isotropic Gaussian distribution derived in Part 1 for the limit $\tau_c \ll \tau_v$, in which the mean-square velocity in the vertical direction is half that in the horizontal plane.

The distribution function for species i, which incorporates the first effect of collisions between particles settling at their terminal velocity, is singular at the terminal velocity, and is non-zero in a finite region of velocity space between the terminal velocities of the two species (see figure 4). The fraction of particles having velocities $O(\exp(-1/\epsilon))$ different from their terminal velocities is $1-O(\epsilon)$, and the fraction of particles having velocities $O(1)$ different from their terminal velocities is $O(\epsilon)$. The skewness in the vertical direction, which the ratio of the third moment to the second moment raised to $\frac{3}{2}$ power, increases as $\epsilon^{-\frac{1}{2}}$ in the limit of small ϵ.

The first corrections to the velocity moments, calculated using the above distribution functions, incorporate the effect of the dispersion of the particle velocities on the collisional transfer rates. The dispersion tends to decrease the magnitude of the velocity moments due to a decrease in both the frequency of collision, and the average difference in the momentum and energy of the two species. These corrections are less than 10% for ϵ_1 between 0.1 and 0.3, indicating that the asymptotic analysis is quite robust in this limit. As the size ratio, a_2/a_1, increases from 0 to 1, the velocity moments of species 1 first increase, due to an increase in the average momentum and energy of species 2, and then decrease, due to a decrease in the collision frequency as the difference in the terminal velocities becomes smaller. For $a_2/a_1 > 1$, the velocity moments increase monotonically as the size ratio increases.

If the collisions between particles are inelastic, the domain of the velocity distribution function shrinks, but the form of the distribution remains the same. The decrease in the mean-square of the fluctuating velocity due to dissipation in inelastic collisions is $O(1-e^2)$. This decrease is small when the coefficient of restitution is close to 1, which is unlike the limit $\tau_c \ll \tau_v$ analysed in Part 1, where inelastic collisions can result in a significant decrease in the fluctuating velocity even when the coefficient of restitution is close to 1.

The qualitative form of the distribution function could be different if the drag force on the particle is not a linear function of its velocity. For example, if the drag force is proportional to the mth power of the velocity, the distribution function is not singular at the terminal velocity for $m > 1$.

The dynamics of a bidisperse suspension of particles in the complementary limit, $\tau_c \ll \tau_v$, was examined in Part 1. Figure 10(*a–c*) compares the mean and mean-square velocities of species 1, non-dimensionalized by $v_{1t}^{\dagger}$ and $v_{1t}^{\dagger 2}$ respectively, in the two limits. The ratio of number densities, n_2/n_1, is 1, and the mean and mean-square velocities are plotted as a function of the dimensionless parameter, ϵ_1, defined as $[n_1(4\pi a_1^2)\, v_{1t}^{\dagger}/\tau_{v1}]$. The limit $\epsilon_1 \ll 1$ ($\tau_v \ll \tau_c$) was analysed in this paper, and the limit $\epsilon_1 \gg 1$ ($\tau_c \ll \tau_v$) was analysed in Part 1. The mean velocity of species 1 is close to its terminal velocity in the limit $\epsilon_1 \ll 1$ and decreases to the mean velocity of the suspension, given by (2.6) in Part 1, as ϵ_1 is increased. The mean-square velocities in the vertical and horizontal directions are small in the two limits, and increase in the intermediate region. The increase is gradual in the limit $\epsilon_1 \ll 1$, but is rather sharp in the limit $\epsilon_1 \gg 1$. It was shown in Part 1 that, in the limit $\epsilon_1 \gg 1$, the higher-order corrections to the velocity moments are of the same order of magnitude as the

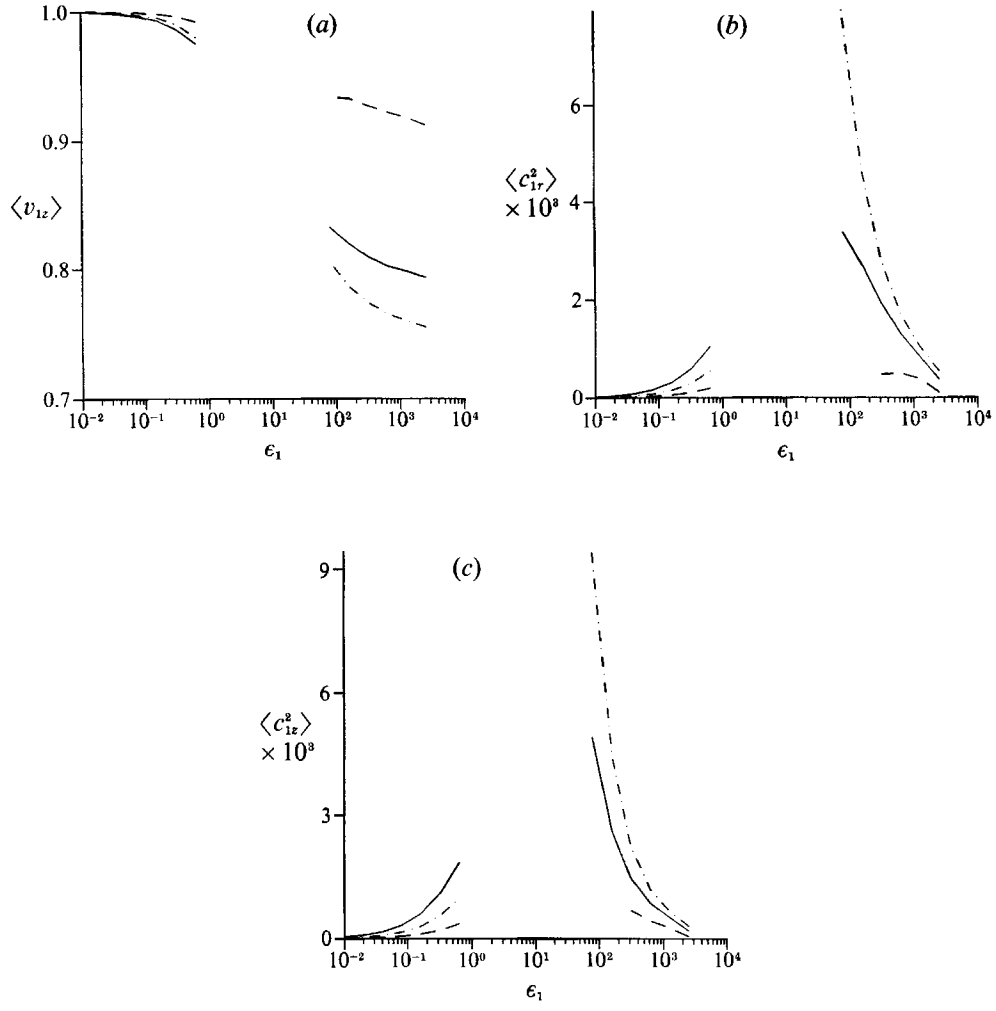

FIGURE 10. (*a*) The mean velocity of particles of species 1 in the vertical direction; (*b*) the mean-square fluctuating velocity of particles of species in the horizontal direction, $\langle c_{1r}^2 \rangle$; and (*c*) the mean-square fluctuating velocity of particles of species 1 in the vertical direction, $\langle c_{1z}^2 \rangle$, all scaled by $v_{1t}^{\dagger 2}$, as functions of ϵ_1. The ratio of number densities is 1. -·-·-·-·-, $a_c = 0.5$; ——, $a_c = 0.7$, – – – – – –, $a_c = 0.9$.

leading terms for ϵ_1 of $O(100)$, and this seems to be the weaker limit in the theory. Therefore, we do not yet have a method of estimating the magnitude of the velocity fluctuations for ϵ_1 of $O(100)$, which is an important parameter range from a practical point of view.

An approximate form for the distribution in between the two limits will be proposed in Kumaran & Koch (1993*b*), and its accuracy will be examined numerically. The form, isotropy and skewness of the distributions in the two limits are very different, and a distribution function that incorporates the features of the distributions in both the limits may find applications in more complicated systems.

The authors thank James T. Jenkins for many helpful discussions. This work was supported by grant CTS-885 7565 from the National Science Foundation's Fluids, Particulates and Hydraulics Program.

Appendix. Effect of hydrodynamic interactions on the variance of the velocity in a polydisperse suspension

In general, two mechanisms create particle velocity fluctuations in a suspension of particles settling through a gas. First, the fluid velocity fluctuations induced by a particle result in a fluctuating force on the surrounding particles; this mechanism was treated for a suspension of monodisperse particles by Koch (1990). In a polydisperse suspension, the differences in the terminal velocities of the different species together with solid–body collisions will create particle velocity fluctuations. In the present work, we have treated the second mechanism, and, for simplicity, neglected the fluid dynamic interactions.

While both sources of particle velocity fluctuations are present in a polydisperse suspension, it may be shown by a slight adaptation of Koch's (1990) arguments that the effects of hydrodynamic interactions are much smaller than the effects of differing terminal velocities in a polydisperse suspension at sufficiently high Stokes number. The contribution of each mechanism to the velocity variance may be estimated as the square of the velocity change in a single interaction multiplied by the rate of interactions and by the viscous relaxation time τ_{vi}. The rate of solid-body collisions between particles settling near their terminal velocities is $O(n_i a_i^2 (v_{1t}^\dagger - v_{2t}^\dagger))$, and the change in the velocity due to a collision is $O(v_{1t}^\dagger - v_{2t}^\dagger)$. Thus, the variance of the velocity due to the effects of polydispersity is $O(n_i a_i^2 (v_{1t}^\dagger - v_{2t}^\dagger)^3 \tau_{vi})$ or $O(v_{it}^{\dagger 2} St\, V (\Delta a/a_i)^3)$, where St is the Stokes number, V is the volume fraction, and Δa is a characteristic difference in particle radii. The last estimate was based on a situation in which the densities of the different species are the same and only their radii differ.

Koch (1990) showed that the fluid dynamic interactions between particles in a gas–solid suspension are like those in a Brinkman fixed bed provided that the viscous relaxation of the particles is small in the time that it takes a particle to translate through a Brinkman screening distance $aV^{-\frac{1}{2}}$. In the present case, this criterion is $\tau_v \gg aV^{-\frac{1}{2}}(v_{1t}^\dagger - v_{2t}^\dagger)^{-1}$, or $St \gg V^{-\frac{1}{2}}(a_i/\Delta a)$. When this criterion is satisfied, we can estimate the contribution of the fluid dynamic interactions to the variance as follows. The most important fluid dynamic interaction occurs at a distance comparable to the screening length $aV^{-\frac{1}{2}}$. The rate at which the particle undergoes such interactions is $O(n_i((v_{1t}^\dagger - v_{2t}^\dagger))(a_i V^{-\frac{1}{2}})^2)$ or $O((v_{1t}^\dagger - v_{2t}^\dagger)/a_i)$. The change in the velocity during an interaction is $O(v'^\dagger \tau_I/\tau_{vi})$ where $v'^\dagger$, the fluid velocity disturbance, is $O(V^{\frac{1}{2}} v_{it}^\dagger)$ and τ_I is the characteristic time of the interaction which is $O(a_i V^{-\frac{1}{2}}/(v_{1t}^\dagger - v_{2t}^\dagger))$. Thus, the change in the velocity during the interaction is $O(v_{it}^\dagger St^{-1}(a_i/\Delta a))$. Combining these factors, the contribution of the fluid dynamic interactions to the particle velocity variance is $O(v_{it}^{\dagger 2} St^{-1}(a_i/\Delta a))$.

From these estimates we see that the effect of solid-body collisions on the particle velocity variance is much larger than that of fluid dynamic interactions if $St \gg V^{-\frac{1}{2}}(a_i/\Delta a)^2$. This means that in a polydisperse suspension, i.e. $\Delta a/a_i \sim O(1)$, the fluid dynamic interactions may be neglected in the limit $St \gg V^{-\frac{1}{2}}$.

Koch's analysis dealt with fluid dynamic interactions between particles in a monodisperse suspension. From the preceding arguments, it is seen that the criterion for neglecting the effects of polydispersity in a nearly monodisperse suspension becomes more stringent with increasing Stokes number. In particular, polydispersity may be neglected only if $\Delta a/a_i \ll St^{-\frac{1}{2}} V^{-\frac{1}{4}}$.

The foregoing discussion applies to a fully polydisperse suspension, which could be characterized by a non-singular distribution function $F(a)$, where $F(a)\,\mathrm{d}a$ is the fraction of particles whose radii are between a and $a+\mathrm{d}a$. This is, of course, the case

of most practical interest. Although it would be straightforward to extend our analysis of solid-body collisions to a fully polydisperse suspension, the analysis in the body of the paper deals with a suspension of only two distinct particle species. Interactions between particles of exactly the same terminal velocity are extremely rare in a polydisperse suspension, but such interactions are common in a bidisperse suspension. Since the period of time which two particles with the same terminal velocity spend undergoing a fluid dynamic interaction is much longer than the interaction time of particles with different terminal velocities, the effects of fluid dynamic interactions between particles of the same species is relatively large.

The effects of fluid dynamic interactions between particles of the same species can be obtained by the direct application of Koch's (1990) results for monodisperse suspensions. For $St \gg V^{-\frac{3}{4}}$, it was shown that each fluid dynamic interaction caused a small change in the particle velocity. As a result, the fluid dynamic interactions were described in terms of a diffusivity in velocity space. The inclusion of such a velocity space diffusivity in the equation (2.5) for the velocity distribution would remove the singularity at $u_i = 0$ in (2.23). Koch (1990) showed that the fluid dynamic interactions led to an $O(v_{1t}^{\dagger 2} St^{-\frac{2}{3}})$ variance in the particle velocity for $St \gg V^{-\frac{3}{4}}$, indicating that the effects of hydrodynamic interactions on the variance of the velocity are small compared with the effects of solid-body collisions for a bidisperse suspension as long as $St \gg V^{-\frac{3}{4}}$.

It seems likely that the effects of hydrodynamic interactions will remain negligible for somewhat lower Stokes numbers as well. Koch (1992) recently demonstrated that the $O(v_{1t}^{\dagger 2} St^{-\frac{2}{3}})$ scaling of the velocity variance in a monodisperse gas–solid suspension holds at smaller Stokes numbers, $1 \ll St \ll V^{-\frac{3}{4}}$, for which a new screening mechanism involving the non-local effective viscosity of the suspension replaces the Brinkman screening. However, while bidispersity will not affect the qualitative nature of the Brinkman screening for $St \gg V^{-\frac{3}{4}}$, we would expect it to affect the screening mechanism for smaller Stokes numbers. Thus, no definite statement can be made at present about the effects of fluid dynamic interactions in a bidisperse suspension for which $St \ll V^{-\frac{3}{4}}$.

REFERENCES

Batchelor, G. K. 1988 A new theory for the instability of a uniform fluidized bed. *J. Fluid Mech.* **193**, 75–110.

Didwania, A. K. & Homsy, G. M. 1982 Resonant sideband instabilities in wave propogation in fluidized beds. *J. Fluid Mech.* **122**, 433–438.

Koch, D. L. 1990 Kinetic theory for monodisperse gas–solid suspension. *Phys. Fluids* A**2**, 1711–1723.

Koch, D. L. 1992 Anomalous diffusion of momentum in a dilute gas–solid suspension. *Phys. Fluids* A**4**, 1337–1346.

Kumaran, V. & Koch, D. L. 1993*a* Properties of a bidisperse particle–gas suspension. Part 1. Collision time small compared with viscous relaxation time. *J. Fluid Mech.* **247**, 623–641.

Kumaran, V. & Koch, D. L. 1993*b* Approximate velocity distribution functions for a bidisperse particle–gas suspension. *Intl J. Multiphase Flow* (submitted).

Lumley, J. L. 1978 Two phase and non Newtonian Flows. In *Turbulence* (ed. P. Bradshaw). Springer.